Earth, Moon, and Planets (2019) 122:73–82
https://doi.org/10.1007/s11038-018-9522-4

# Distinction in the Interplanetary Characteristics of Accelerated and Decelerated CMEs/Shocks

**K. Suresh[1] · A. Shanmugaraju[2] · Y.-J. Moon[3]**

Received: 5 April 2018 / Accepted: 27 November 2018 / Published online: 5 December 2018


**Abstract**
A set of 58 Coronal Mass Ejections (CMEs) with different kinematics near the sun in LASCO Field of view (FOV) is classified into two groups (i) CMEs which are accelerating (group-I) and (ii) CMEs which are decelerating (group-II). We analyze their interplanetary propagation characteristics to study the distinction between these two groups of events. Some of the following deviations are noted between the two groups as: (i) While group-II events have greater mean values of Standoff distance, Standoff time than the group-I events, the mean transit times of ICMEs and IP shocks are relatively lower for them. (ii) Group-II events are more (30%) radio-rich than the group-I (10%) and they are associated with type II solar radio burst in lower corona, (iii) The possibility of having excess magnetic energy that supports the propagation of CMEs to some extent is studied using estimated speed ($V_{EST}$) and it is found that a slightly more number of events in group-I (48%) has $V_{EST} > V_{LASCO}$ than group-II (33%). (iv) Net interplanetary acceleration is positive for 35% and 19% in group-I and group-II events respectively. (v) It is also found that ICME/IP shock characteristics of the two groups depend strongly on the CME acceleration.

**Keywords** CME · ICME · IP shock

## 1 Introduction

Coronal mass ejections (CMEs) are large-scale plasma structures that erupt from closed magnetic field regions on the sun and travel through ambient medium. During its propagation, it interacts with the solar wind and causes fast mode magneto hydrodynamic

✉ K. Suresh
mrsuresh555@gmail.com

A. Shanmugaraju
ashanmugaraju@gmail.com

Y.-J. Moon
moonyj@khu.ac.kr

[1] Department of Physics, Rathinam Technical Campus, Coimbatore, India

[2] Department of Physics, Arul Anandar College, Karumathur, 625 514 Madurai, India

[3] School of Space Research, Kyung Hee University, Yongin 446-701, Republic of Korea

(MHD) shock. This shock accelerates the charged particles to very high energies (Gopalswamy et al. 2009). When these shocks travel through ambient medium, it excites the non-thermal electrons, and they are then converted and observed as radio waves (Nelson and Melrose. 1985; Cairns et al. 2003; Mann et al. 2003; Cho et al. 2005). Type II bursts are a type of solar radio burst with slow drift in radio spectrum. Since the type II radio bursts are earlier indicator of the shocks, it gives the observational details of the shocks before it attains at 1AU. Shock wave observed at 1 AU show a direct association with the CME from the sun (Manoharan et al. 2004). Interplanetary (IP) shocks at 1 AU have association with large space-weather effects such as, Sudden Storm Commencement (SSC) and geomagnetic storms. CMEs that are faster than solar wind decelerates and slower ones accelerate in LASCO field of view (FOV). At the beginning, it undergoes a rapid acceleration and reaching a maximum acceleration in the inner corona before being controlled by the aerodynamic drag (Wood et al. 1999; Gopalswamy and Thompson 2000; Zhang et al. 2001; Vršnak 2001; Vrsnak et al. 2013). Moon et al. (2002) proposed evidences for two distinct types of CMEs which are subjected to different kinematics. CMEs propagate into interplanetary space with velocities of a few hundred to a few thousand km/s (e.g., Yashiro et al. 2004) and may cause severe space weather effects and geomagnetic storms when interacting with the Earth's magnetic field (see e.g., Schwenn 2006; Pulkkinen 2007 and references therein). There are many authors who studied about the CME and its interplanetary counterparts (Chen 1996; Gopalswamy et al. 2001; Manoharan et al. 2004; Gopalswamy et al. 2005; Manoharan 2006; Shanmugaraju et al. 2009; Manoharan and Mujiber Rahman 2011; Vasanth et al. 2015; Shanmugaraju et al. 2018).

Manoharan and Mujiber Rahman (2011) discussed about the propagation of CME with its internal magnetic energy, and the energy dissipation with two step deceleration of CME speed profile from Sun to 1 AU. That is, the low or moderate deceleration is within 0.5 AU and a rapid deceleration at further distance, (Chen 1996; Tokumaru et al. 2000; Manoharan 2006; Howard et al. 2007). They also studied about the energy involved to overcome the drag force that transferred to the solar wind in at least 50% of events.

Sheeley et al. (1999) and Dal Lago et al. (2004) investigated some events based on acceleration and deceleration, and concluded that the acceleration process is closely related to CME formation whereas the deceleration is related to the interaction of CME with the ambient medium. Yurchyshyn et al. (2005) studied the speed distribution of 4315 CMEs based on their acceleration and deceleration behavior. They found that the same driving mechanism of a nonlinear nature is acting on both slow and fast CMEs. Gao and Li (2009) investigated the cyclic evolutionary behavior of CME acceleration for accelerating and decelerating CME events in solar cycle 23. They also found that the different driving mechanisms of accelerating and decelerating events such as the drag force dominate the CMEs during solar maximum whereas propelling force dominates the CMEs at the rest of time interval.

Shen et al. (2012) analyzed the forces which are responsible for the acceleration and deceleration of CMEs, and its momentum exchange with solar wind. They reported that magnetic pressure (in terms of Lorentz force) and pressure gradient are responsible for the acceleration of CME whereas the forces which cause the deceleration of CMEs are aerodynamic drag, the Sun's gravity and the tension of magnetic field. Michalek et al. (2004) obtained different equations for acceleration in terms of CME's initial speed for normal and extreme events for determining the travel time. Following this, Syed Ibrahim and Shanmugaraju (2006) utilized these equations and found that each CME behaves differently in the IP medium.

Hence, the study of CMEs and their associated shock based on their acceleration behavior is necessary to understand its evolution from corona to interplanetary space. In this paper, we studied the propagation characteristics of the ICMEs/shocks for accelerating and decelerating CMEs separately. Data selection is given below in Sect. 2. The results are presented and discussed in Sect. 3, and a summary is given in Sect. 4.

## 2 Data Selection

We collect 184 interplanetary coronal mass ejections (ICMEs) from Richardson/Cane catalogue (www.srl.caltech.edu/ACE/ASC/DATA/level3/icmetable2. Html, Cane and Richardson 2003) from 2005 to 2014 for this study and We select 58 events based on the criteria that these events must have IP shock signature at 1AU and should have association with LASCO CMEs. Based on their acceleration behavior in LASCO FOV (2-30Ro, Brueckner et al. 1995), we divided these events into two categories. They are (i) ICMEs associated with accelerating CMEs in LASCO FOV (group-I) and (ii) ICMEs associated with decelerating CMEs in LASCO FOV (group-II). There are 31 and 27 events in group-I and group-II respectively. We neglect the events with less than four height-time data points in the LASCO FOV. We obtain start and end times, speed, intensity of storm in Dst and magnetic field of ICMEs from the Richardson/Cane catalogue. The first detection time and speed of CME are obtained from SOHO/LASCO catalogue (http://cdaw.gsfc.nasa.gov/CME_list/, Yashiro et al. 2004). The IP acceleration can be calculated from the speed difference ($V_{CME} - V_{ICME}$) divided by CME transit time ($T_{CME\ onset} - T_{IP\ shock\ onset}$). The standoff time (SOT) is calculated from the time difference between ICME and IP shock arrival times (http://nssdc.gsfc.nasa.gov/omniweb), and the standoff distance (SOD) is calculated by multiplying SOT with ICME speed (Manoharan and Mujiber Rahman 2011; Mujiber Rahman et al. 2012, 2013).

## 3 Results and Discussion

### 3.1 Properties

We analyze the general properties of two groups of CME events. Interestingly, both the groups contain slow, medium and fast CMEs. Based on the preliminary analysis, some differences are found in the initial speed of CME ($V_{LASCO}$), speed of ICME ($V_{ICME}$) and speed of IP shock ($V_{IP\ shock}$), transit time of ICME and IP shock ($T_{ICME}$ & $T_{IP\ shock}$), standoff time (SOT), standoff distance (SOD) and IP acceleration. The mean values of $V_{LASCO}$, SOT, SOD and IP acceleration are relatively greater for group-II events. However, the transit time of ICME's and IP shocks are larger for group-I events. Number of halo events is almost same for both the groups (68% & 78% for group-I and group-II respectively). Statistical values of general properties of 58 events are listed in Table-1 according to their group. The mean, median and standard deviation of these events are given in columns 2–4 respectively for group-I and for group-II, they are given in columns 5–7. The *P* value of statistical significance is given in the last column.

SOT is the time difference between the arrival times of ICME and IP shock at 1AU. This indicates the temporal association of IP shock and its driver CME (in case of CME-driven). Manoharan and Mujiber Rahman. (2011, herein after referred as paper-1) found

**Table 1** General properties of ICME/IP shocks (bold letters show the difference in the mean values between two groups is statistically significant)

| Properties (58 events) | Group-I (31 events) | | | Group-II (27 events) | | | *P*-value |
|---|---|---|---|---|---|---|---|
| | Mean | Median | SD | Mean | Median | SD | |
| **$V_{LASCO}$ (km $s^{-1}$)** | **703** | **575** | **439** | **895** | **712** | **546** | **0.07** |
| $V_{ICME}$ (km $s^{-1}$) | 449 | 430 | 088 | 481 | 460 | 101 | 0.10 |
| $V_{IP\ shock}$ (km $s^{-1}$) | 465 | 448 | 082 | 499 | 465 | 123 | 0.10 |
| **$T_{ICME}$ (hours)** | **82.2** | **83.9** | **17.6** | **75.8** | **72.8** | **17.8** | **0.09** |
| **$T_{IP\ shock}$ (hours)** | **70.26** | **70.48** | **17.28** | **61.36** | **64.42** | **17.97** | **0.06** |
| **SOD ($R_\odot$)** | **26** | **24** | **13** | **32** | **28** | **16** | **0.06** |
| SOT (hours) | 11.6 | 10 | 5.8 | 13 | 12 | 6 | 0.11 |
| **IP acceleration (m $s^{-2}$)** | **−1.08** | **−0.56** | **1.87** | **−1.90** | **−1.11** | **2.76** | **0.09** |

that the SOT range is between 1 to 25 h for 91 earth-directed events. Mujiber Rahman et al. (2012) found the SOT ranges between 2 to 20 h with a mean value 11.59 h. The SOT calculated in this study ranges from 3 to 26.05 h with a mean value of 11.55 h for group-I and 3.23 to 28 h with a mean value of 13.53 h for group-II events. These values are consistent with the above literature. Note that the mean value of SOT is smaller for group-I events. This implies the closer association of IP shock with the ICME of group-I events rather than group-II events.

Figure 1 (left) shows the heliographic distribution of group-I and group-II events. It is noted that many of the events (62%) occurred in the western region of the sun. It indicates the possibilities of ICME/IP shock reaching the earth. Figure 1 (right) shows the histogram distribution of SOD of 58 events. SOD basically indicates the spatial relationship between driver CME and its associated shock. If it is larger, the relationship between CME and shock is poor and vice versa. From this figure, it is notable that the SOD peaks at 11–20 $R_\odot$ for group-I, but at 21–30 $R_\odot$ for group-II events and the mean values of SOD are 26 $R_\odot$ and 32 $R_\odot$ respectively for group-I and II events. i.e., The average SOD is relatively greater

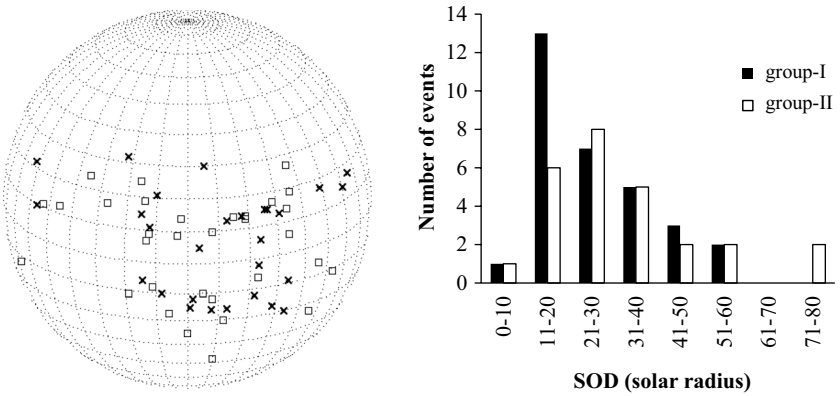


**Fig. 1** (left) Heliographic distribution of group-I (cross symbol) and group-II (square symbol) events (North is at the top and east is at left), (right) distribution of number of events as a function of SOD

for group-II than group-I. However, this difference has statistical significance with P-value of 0.06. The SOD is in the range of 7 $R_\odot$ to 58 $R_\odot$ with a mean value of 26 $R_\odot$ for group-I and 8 $R_\odot$ to 76 $R_\odot$ with a mean value of 32 $R_\odot$ for group-II events. Mujiber Rahman et al. (2013) found that the SOD ranges between 1 to 50 $R_\odot$ with a mean value 29.06 $R_\odot$. The mean values obtained in the present work are consistent with the above literature.

From both spatial and temporal analyzes, we conclude that the group-II events have less amount of sufficient energy to drive and sustain shocks ahead of it near the earth. Hence, more fraction of events in group-I may drive and sustain the shock to a larger distance relative to group-II events.

Though we have classified the 58 events based on their acceleration behavior in LASCO FOV, their acceleration need not be same as positive or negative throughout the sun-earth distance. It may be influenced by the drag force in its latter part of propagation (Vršnak 2001). So, we found the IP acceleration for these 58 events. IP acceleration is more negative for group-II than group-I. In both groups, most of the events (20 in group-I and 22 in group-II) are found to be decelerated whreas few events are accelerated in the IP medium. However, the fraction of positively accelerated events is slightly larger for group-I (35%) than for group-II (19%).

Next, we find the association between CME and the corresponding ICME/IP shock by studying the metric, DH and IP type II bursts. The type II solar radio bursts can be observed in metric and Deca-Hectometric (DH) region. Ground based radio telescopes are used for observing the type II bursts at metric wavelength from 350 MHz to 30 MHz. Since the ionospheric cut-off frequency is 30 MHz, we cannot observe the type II bursts beyond this wavelength. So, we use the space-borne radio telescopes to observe these solar radio bursts. The association of metric type II bursts with these 58 events were checked with the data from Green Bank Solar Radio Burst Spectrometer (http://www.astro.umd.edu/~white/gb/) and the DH type II association were checked with the WIND spacecraft data (https://cdaw.gsfc.nasa.gov/CME_list/radio/waves_type2.html). In group-I, only 10% of events are associated with the type II burst in metric and DH region, but 30% of events having such association in group-II. This means that more fraction of group-II events are radio rich in lower corona and in IP medium than the group-I events. Gopalswamy et al. (2010) found that the RQ CMEs were generally accelerating within the coronagraph field of view, whereas RL CMEs were decelerating. This is consistent with the above results obtained here.

### 3.2 Estimated Speed and Internal Energy

CMEs originate from the sun and propagate through the interplanetary (IP) medium. During their propagation, its speed decreases as it goes away from the sun, and finally reaches the speed of the background solar wind. As we know, high speed CME events should arrive at earth soon. But this may not be the case for all the CMEs. Some CMEs take longer transit time to reach earth although it has high speed near the sun. So, we derive estimated initial speed ($V_{EST}$) as instructed in paper-1. If the estimated speed is greater than the initial speed, then that CME event is expected to be arrive at earth soon. The estimated initial speed ($V_{EST}$) can be calculated from the following relation $V_{AVG} = \left(\frac{V_{EST}+V_{ICME}}{2}\right)$ (see paper-1) whereas the average speed ($V_{AVG}$) is calculated using CME travel time to 1 AU.

In this study, the average observed initial speeds ($V_{LASCO}$) are 709 km $s^{-1}$ and 926 km $s^{-1}$ for group-I and group-II respectively, and 645 km $s^{-1}$ and 707 km $s^{-1}$ indicate

the average estimated speed ($V_{EST}$) of CMEs in group-I and group-II respectively. In both the groups, the $V_{EST}$ and $V_{LASCO}$ speeds are greater than the ambient solar wind speed.

In paper-1, 91 earth-directed CME events were analyzed. The link between travel time to 1AU and effective acceleration in sun-earth distance was carried out. As stated in that paper, the greater speed of $V_{EST}$ relative to $V_{LASCO}$ tends to have the excess energy to overcome the drag force in IP medium whereas events having lesser speed of $V_{EST}$ tend to decelerate in Sun-Earth distance. From Fig. 2 (left), around 48% of events have greater $V_{EST}$ in group-I. Among these 48% events, four events having speed less than the average solar wind speed 450 km/s and they might have been accelerated by the solar wind. Remaining 12 events for which $V_{EST} > 450$ km/s might have an excess of energy associated with the CME. On the other hand, in Fig. 2 (right), about 31% of events have greater $V_{EST}$ and 69% of events have lesser $V_{EST}$. Since many of the group-II events show $V_{EST} < V_{INT}$, these events are not supposed to overcome the drag force. In other words, these events are likely to decelerate in Sun-Earth distance.

### 3.3 Effects of Initial Acceleration

The initial kinematics of CMEs are studied using acceleration- speed relation of CMEs in the LASCO FOV. In this section, first we relate the CME properties in the LASCO FOV such as initial acceleration (a) and the speed (v) as shown in Fig. 3. From these plots, it can be understood that the a-v relation is distinct for the two groups. The initial speeds when $a = 0$ are quite different: 430 km/s and 588 km/s for accelerating and decelerating groups of CMEs, respectively. It is consistent with the literature that slower CMEs are accelerated and faster CMEs are decelerated. From Fig. 3b, it can be noted that 13.5 m/s2 and -8.0 m/s2 are acceleration of group-I and group-II respectively. These values are the results of the combination of effects due to drag/push force of the ambient solar wind and Lorentz force of magnetic energy of the CME.

Gopalsawamy et al. (2012) explained the acceleration tendency of fast and slow CMEs with respect to the critical solar wind speed (Fig. 2). As he stated, If the speed of the CME is less than the critical solar wind speed, then that the event tends to accelerate whereas the event with higher speed tends to decelerate. In this paper, Fig. 3 supports the above statement. The straight-line fitting obtained for group-I is $y = 0.032x - 7.965$ and for group-II is $y = 0.033x + 13.51$. By setting "y" value as zero, then we get the critical speed for

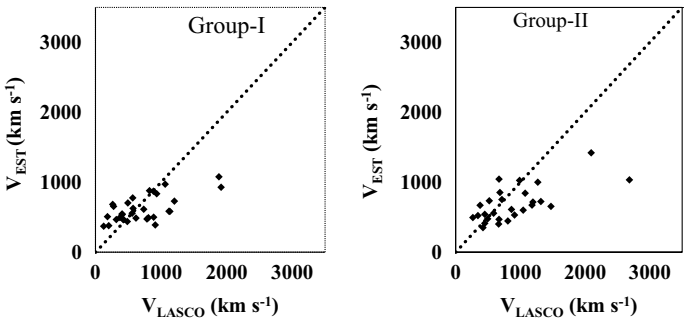


**Fig. 2** Correlation shows the positive trend between observed initial speed ($V_{LASCO}$) and estimated initial speed ($V_{EST}$). The dashed line indicates 100% correlation between these two parameters

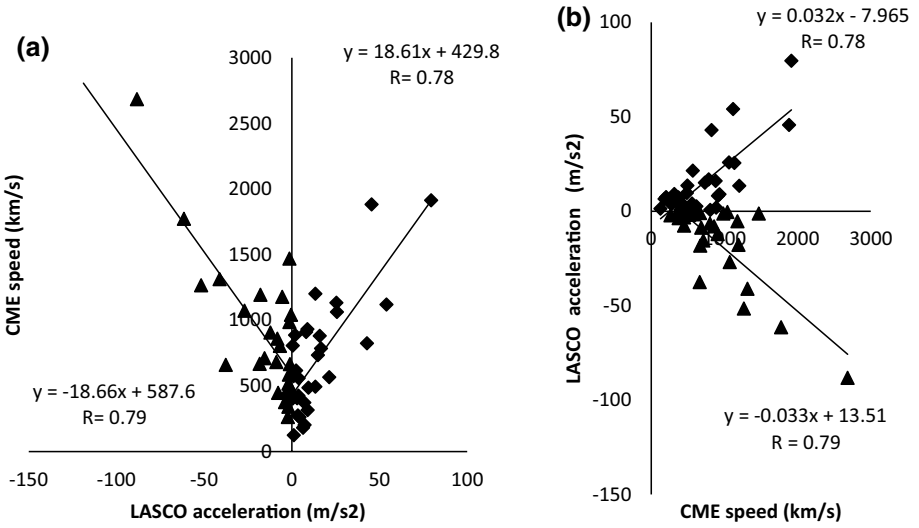


**Fig. 3** **a** Acceleration—speed relation for both groups: diamond—group I, triangle—group II. The axes are just interchanged in (**b**). Linear fitting to the data points is shown by a straight line

group-I is 248 km/s and 409 km/s. Hence the group-I events accelerate and group-II events decelerate.

Then the dependency of transit time, speed and IP acceleration of the ICMEs/IP shocks on the acceleration is studied. The initial acceleration in the LASCO FOV is plotted against transit time of ICME and IP shock for both groups in Fig. 4. From this figure, though the trend seem similar for both groups, the correlation is slightly better for group I. Also, the group-I events seem to take longer time to reach earth when compared to group-II events. More interesting point is that the transit time is lesser for highly decelerating or highly accelerating CMEs. It is also evident in case of transit time of IP shock as in Fig. 4b.

The dependence of speed and interplanetary acceleration of ICMEs on the initial acceleration is shown in Fig. 5 a, b respectively. Both these plots show clear dependency and the correlation coefficient values are nearly similar for both the groups. From these two plots, the distinct characteristics near the sun (initial speed and acceleration) of majority events from both groups change to similar characteristics (speed and IP acceleration) of ICMEs. Recently, Sachdeva et al.(2017) analysed dynamics of 38 events and found that the Lorentz magnetic force becomes negligible within 4 solar radii for fast CMEs, but it becomes effective up to 12–50 solar radii for slow CMEs.

## 4 Summary

We have investigated 58 CME events and their interplanetary counterparts such as ICMEs and IP shocks. Based on their distinct acceleration behavior near the sun, we classified these events into two groups such as accelerating (group-I) and decelerating (group-II). The source distribution of 58 events on the sun shows the greater possibilities of western events (62% of events) reaching the earth.

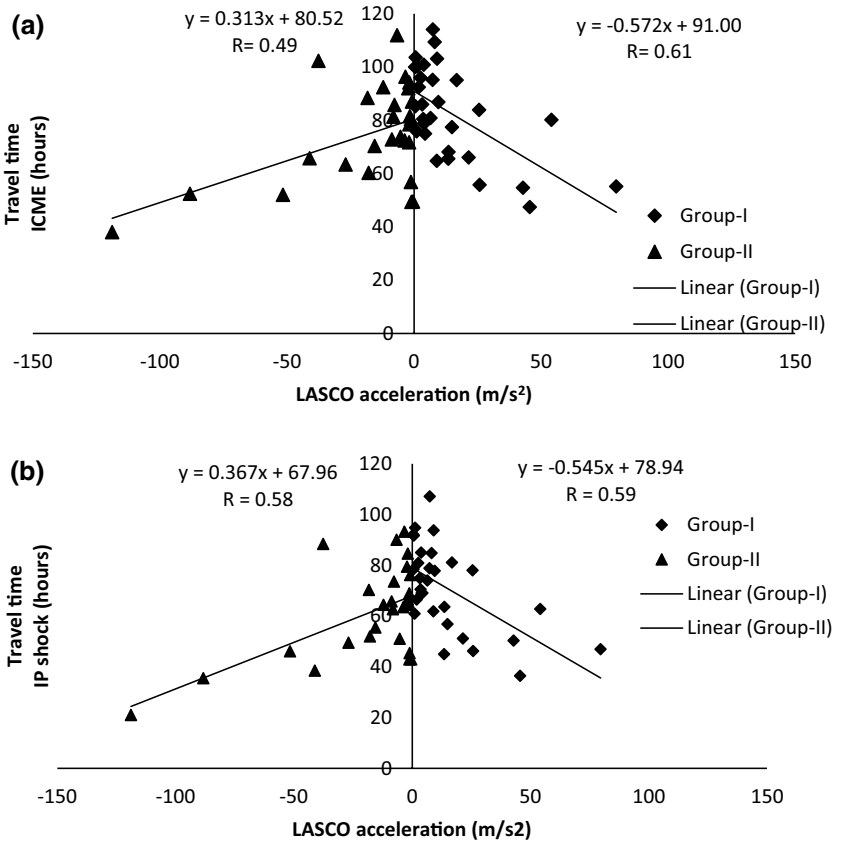


**Fig. 4** Transit times of ICME (**a**) and IP shock (**b**) are plotted against LASCO acceleration for both groups. Linear fitting to the data points is shown by a straight line

There are some differences noted between the two groups as follows: (i) The physical properties of group-II events such as $V_{LASCO}$, SOT, SOD and IP acceleration are found to be greater for group-II events. (ii) On the other hand, the transit time of ICMEs/IP shocks of group II events is slightly lesser. (iii) The transit time of ICME/IP shock is lesser for either highly decelerating or highly accelerating CMEs. (iv) Among the total 58 events, 10% and 30% of events are associated with the type II burst in metric and DH region in group-I and group-II respectively. This implies that more fraction of group-II events become radio rich in lower corona and in IP medium than group-I. (v) In the near-earth region, net interplanetary acceleration is positive for 35% and 19% in group-I and group-II events respectively. i.e., the number of positively accelerated events is higher in group-I in near-earth region. (vi) The high correlations obtained between the acceleration and other properties of CMEs/ICMEs reveal their dependency.

In general, SOD and SOT indicates the spatial and temporal relationship between driver CME and its associated shock. The higher values of both SOD and SOT of group-II reveal that these events have less amount of sufficient energy to drive and sustain shocks ahead of it in near-earth region. Group-I events having less SOD and SOT indicates that it drives and sustains the shock to a larger distance than group-II events.

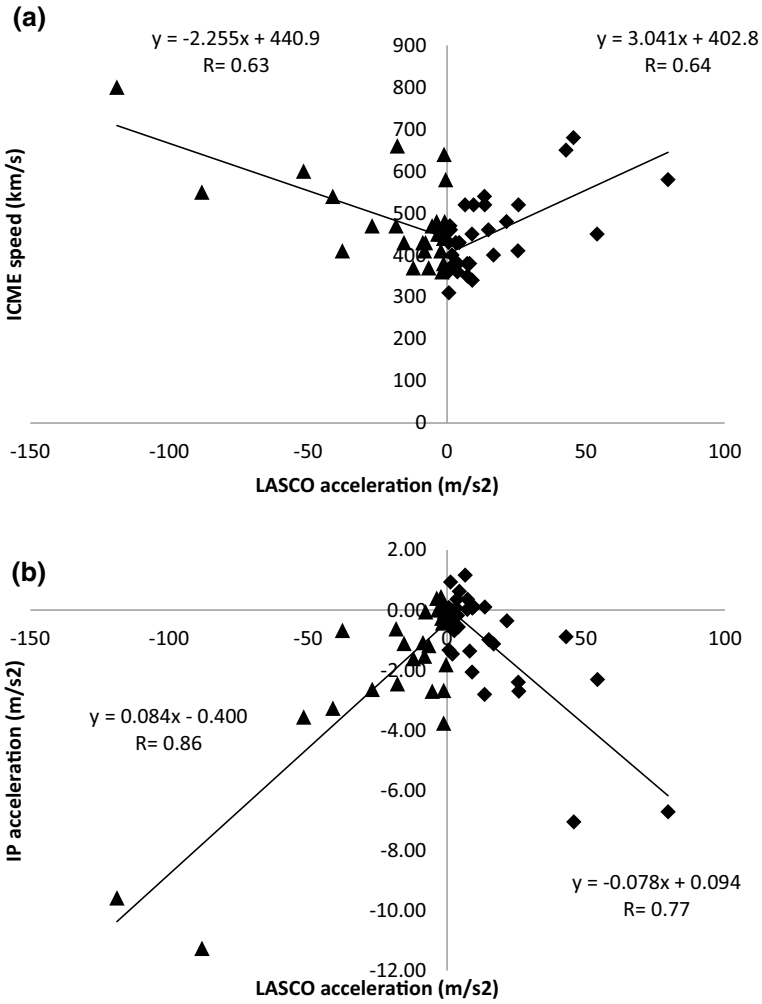


**Fig. 5** Speed (**a**) and IP acceleration (**b**) of ICME are plotted against LASCO acceleration for both groups. Linear fitting to the data points is shown by a straight line

Otherwise, the high speed CME events tend to decelerate heavily in sun-earth distance and the CME speed reduces significantly. This lower speed would have caused larger SOD. This may be the reason for the high speed (greater $V_{INT}$) events having larger SOD at 1AU.

The events with $V_{EST} > V_{LASCO}$ have lower SOT and this implies that the close association of CME driver to the shock. The number of events which has $V_{EST} > V_{LASCO}$ is higher in group-I. This statement also supports the group-I events drive and sustain the shock very closely than group-II events. Around 48% and 33% of events have greater $V_{EST}$ in group-I and group-II respectively. In group-I, among these 48% events, four events (having speed less than the average solar wind speed 450 km/s) might have been accelerated by the solar wind. It means that the remaining CME events have an excess of internal energy. In group-II, about 33% of events have greater $V_{EST}$ and 67% of events have lesser $V_{EST}$. Many of the

group-II events showing $V_{EST} < V_{INT}$ are not capable to overcome the drag force. In other words, these events are likely to decelerate in the Sun-Earth distance.

## References


G.E. Brueckner, R.A. Howard, M.J. Koomen, C.M. Korendyke, D.J. Michels, J.D. Moses, D.G. Socker, K.P. Dere, P.L. Lamy, A. Llebaria, M.V. Bout, R. Schwenn, G.M. Simnett, D.K. Bedford, C.J. Eyles, Sol. Phys. **162**, 357 (1995)

H.V. Cane, I.G. Richardson, J. Geophy. Res. (2003). https://doi.org/10.1029/2002ja009817

I.H. Cairns, S.A. Knock, P.A. Robinson, Z. Kuncic, Space Sci. Rev. **107**, 27 (2003)

J. Chen, J. Geophys. Res. **101**, 27499–27520 (1996)

K.-S. Cho, Y.-J. Moon, M. Dryer, A. Shanmugaraju, C.D. Fry, Y.-H. Kim, S.-C. Bong, Y.-D. Park, J. Geophys. Res. **110**, A12101 (2005)

A. Dal Lago, L.E.A. Vieira, E. Echer, W.D. Gonzalez, A.L.C. de Gonzalez, F.L. Guarnieri, N.J. Schunch, R. Schwenn, Sol. Phys. **222**, 323 (2004)

P.X. Gao, K.J. Li, Acta Astronomica Sinica. **50**, 383 (2009)

N. Gopalswamy, B.J. Thompson, J. Atmos. Sol. Terr. Phys. **62**, 1457 (2000)

N. Gopalswamy, A. Lara, S. Yashiro, M.L. Kaiser, R.A. Howard, J. Geophys. Res. **106**, 29207 (2001)

N. Gopalswamy, A. Lara, P.K. Manoharan, R.A. Howard, Adv. Space Res. **36**, 2289 (2005)

N. Gopalswamy, W.T. Thompson, J.M. Davila, M.L. Kaiser, S. Yashiro, P. Mäkelä, G. Michalek, J.-L. Bougeret, R.A. Howard, Sol. Phys. **259**, 227 (2009)

N. Gopalswamy, H. Xie, P. Makela, S. Akiyama, S. Yashiro, M.L. Kaiser, R.A. Howard, J.-L. Bougeret, Astrophys. J. **710**, 1111 (2010)

N. Gopalswamy, N. Nitta, S. Akiyama, P. Makela, S. Yashiro, Astrophys. J. **744**, 72 (2012)

T.A. Howard, C.D. Fry, J.C. Johnston, D.F. Webb, Astrophys. J. **667**, 610–625 (2007)

G. Mann, A. Klassen, H. Aurass, H.-T. Classen, Astron. Astrophys. **400**, 329 (2003)

P.K. Manoharan, Sol. Phys. **235**, 345 (2006)

P.K. Manoharan, N. Gopalswamy, S. Yashiro, A. Lara, G. Michalek, R.A. Howard, J. Geophys. Res. **109**, A06109 (2004)

P.K. Manoharan, R. Mujiber, J. Atmos. Sol. Terr. Phys. **73**, 671 (2011)

G. Michalek, N. Gopalswamy, A. Lara, P.K. Manoharan, Astron. Astrophys. **423**, 729 (2004)

Y.-J. Moon, G.S. Choe, Y.J. Moon, H. Wang, Y.D. Park, N. Gopalswamy, G. Yang, S. Yashiro, Astrophys. J. **581**, 694–702 (2002)

A. Mujiber Rahman, S. Umapathy, A. Shanmugaraju, Y.J. Moon, Adv. Space Res. **50**, 516 (2012)

A. Mujiber Rahman, A. Shanmugaraju, S. Umapathy, Y.-J. Moon, J. Atmos. Sol.-Terr. Phys. **105**, 181 (2013)

G.J. Nelson, D.B. Melrose, in *Solar Radiophysics*, ed. by D.J. McLean, N.R. Labrum (Cambridge University Press, Cambridge, 1985), p. 350

T. Pulkkinen, Living Rev. Sol. Phys. **4**, 1 (2007)

N. Sachdeva, P. Subramnaian, A. Vourlidas, V. Bothmer, Sol. Phys. **292**, 118 (2017)

R. Schwenn, Living Rev. Sol. Phys. **3**, 1 (2006)

A. Shanmugaraju, Y.-J. Moon, B. Vrsˇnak, D. Vrbanec, Sol. Phys. **257**, 351–361 (2009)

A. Shanmugaraju, K. Suresh, V. Vasanth, G. Selvarani, S. Umapathy, Astrophys. Space Sci. **363**, 126 (2018)

N.R. Sheeley, J.H. Walters, Y.-M. Wang, R.A. Howard, J. Geophys. Res. **104**, 24739 (1999)

F. Shen, S.T. Wu, X. Feng, C.C. Wu, J. Geophys. Res. **117**, A11101 (2012)

K. Suresh, A. Shanmugaraju, M. Syed Ibrahim, Astrophys. Space Sci. (2006). https://doi.org/10.1007/s10509-016-2944-4

M. Tokumaru, M. Kojima, K. Fujiki, A. Yokobe, J. Geophys. Res. **105**, 10435 (2000)

V. Vasanth, Y. Chen, X.L. Kong, B. Wang, Sol. Phys. **290**, 1815 (2015)

B. Vršnak, Sol. Phys. **202**, 173 (2001)

B. Vršnak, T. Žic, D. Vrbanec et al., Sol. Phys. **285**, 295 (2013). https://doi.org/10.1007/s11207-012-0035-4

B.E. Wood, M. Karovska, J. Chen, G.E. Brueckner, J.W. Cook, R.A. Howard, Astrophys. J. **512**, 484 (1999)

S. Yashiro, N. Gopalswamy, G. Michalek, O.C. St. Cyr, S.P. Plunkett, N.B. Rich, R.A.A. Howard, J. Geophys. Res. **109**, A07105 (2004)

V. Yurchyshyn, S. Yashiro, V. Abramenko, H. Wang, N. Gopalswamy, Astrophys. J. **619**, 599 (2005)

J. Zhang, M.R. Kundu, S.M. White, K.P. Dere, J.S. Newmark, Astrophys. J. **561**, 396 (2001)